

Thermalization in many-fermion quantum systems with one- plus random k -body interactions

Priyanka Rao* and N. D. Chavda†

*Department of Applied Physics, Faculty of Technology and Engineering,
The Maharaja Sayajirao University of Baroda, Vadodara-390001, India*

arXiv:2206.10467v2 [nlin.CD] 25 Feb 2023

Abstract

We study the mechanism of thermalization in finite many-fermion systems with random k -body interactions in presence of a mean-field. The system Hamiltonian H , for m fermions in N single particle states with k -body interactions, is modeled by mean field one-body $h(1)$ and a random k -body interaction $V(k)$ with strength λ . Following the recent application of q -Hermite polynomials to these ensembles, a complete analytical description of parameter q , which describes the change in the shape of state density from Gaussian for $q = 1$ to semi-circle for $q = 0$ and intermediate for $0 < q < 1$, and variance of the strength function are obtained in terms of model parameters. The latter gives the thermalization marker λ_t defining the thermodynamic region. For $\lambda \geq \lambda_t$, the smooth part of the strength functions is very well represented by conditional q -normal distribution (f_{CN}), which describes the transition in strength functions from Gaussian to semi-circle as the k -body interaction changes from $k = 2$ to m in H . In the thermodynamic region, ensemble averaged results for the first four moments of the strength functions and inverse participation ratio (IPR) are found to be in good agreement with the corresponding smooth forms. For higher body rank of interaction k , system thermalizes faster.

Keywords: Random matrix theory and extensions, Quantum chaos, Quantum Thermalization, Connections between chaos and statistical physics

I. INTRODUCTION

The onset of thermalization in isolated many-body quantum systems, due to inter-particle interaction between their constituents, has received considerable interest since quite a long time and is now an important research area [1–7]. The connection between the mechanism that leads to thermalization in many-body quantum systems and the onset of quantum chaos, when inter-particle interactions are strong enough, is well established [8–10]. In 1995 using ultra-cold atomic gases, Bose-Einstein condensation (BEC) was achieved for the first time in laboratory [11–13]. Subsequently experiments on cooling and trapping of ultracold atomic gases [14, 15] and electrons in solids[16] developed tremendously, along with important numerical algorithms and techniques to study the dynamics of these isolated quantum

* pnrao-apphy@msubaroda.ac.in

† Corresponding author; ndchavda-apphy@msubaroda.ac.in

systems. This experimental progress facilitates one to artificially simulate these isolated systems and also control the interaction strength by which transition between different quantum phases can be studied [17]. Now, it is clear that the lack of thermalization in many-body interacting systems is due to the emergence of extensively many local integrals of motion, a phenomenon called many-body localization. While on the other hand, the thermalization in non-integrable quantum systems occurs due to the underlying mechanism called the eigenstate thermalization hypothesis (ETH) [18]. ETH essentially means the condition where the individual eigenstates of a many-body interacting system can be treated as (quasi)random superposition of a large number of the basis states [19–23] and then the expectation values of typical observables in the eigenstates follow ergodicity principle. Therefore, the study of mechanism of thermalization in terms of properties of chaotic eigenstates has also received considerable importance [10, 21, 24, 25] rather than the thermalization itself which is defined according to quantities such as temperature, thermodynamic entropy, or/and time relaxation to the steady-state distribution. Many groups have addressed the problem of the emergence of thermalization in many-body quantum systems using different models and studied various aspects related to the role of localization and chaos, statistical relaxation, eigenstate thermalization and ergodicity principle [5, 10, 18, 20, 26–31].

In the past, thermalization in fermion and boson systems have been studied in detail using two-body ($k = 2$) random embedded Gaussian orthogonal ensemble in presence of a mean field [denoted as EGOE(1+2)] [22, 30–35] as they form generic models for finite isolated interacting many-particle (fermions or bosons) systems. Going beyond this, the higher body interactions ($k > 2$) are found to play an important role in various fields like nuclear physics [37], strongly interacting quantum systems [38, 39], in quantum transport in disordered networks connected by many-body interactions [40–42] and also in quantum black holes [43, 44] and wormholes [45] with Sachdev–Ye–Kitaev (SYK) model. This leads to the recent enhance of interest in random matrix ensembles in many-particle spaces generated by random k -body ($k > 2$) interactions in presence of a mean-field recently and they are denoted by EGOE(1+ k) [25, 46–49]. In the strong interaction domain the EGOE(1+ k) reduces to EGOE(k) and these ensembles generate Gaussian to semi-circle transition in the eigenvalue density as body rank k of the interaction changes from 1 to m [50, 51].

Recently, the embedded ensembles with higher k -body interactions are analyze by employing q -Hermite polynomials [25, 46–49]. The use of q -Hermite polynomials in embedded

ensembles appears due to the recent work by Verbaarschot et al on the study of spectral density using SYK models, which are embedded ensemble models of Majorana fermions [43, 52, 53]. It has been demonstrated that the q -normal distribution f_N , which is the weight function for q -Hermite polynomials [54], can be used to describe the smooth form of spectral density in EGOE(k) [25, 46]. Further, the formulae for q -parameter in terms of model parameters N , m and k are derived for fermion as well as boson systems for both EGOE(k) and their Unitary variants EGUE(k) [46]. Very recently, the condition of thermalization is studied in many-body bosonic systems with k -body interaction modeled by EGOE($1+k$) in terms of properties of chaotic wave-function and the formula for thermalization marker λ_t in terms of model parameters is derived [25]. Also, it is shown that [25] in the strong interaction domain ($\lambda \gg \lambda_t$), the strength functions (also known as local density of states) make transition from Gaussian to semi-circle as the rank of interaction k increases in EGOE($1+k$) and their smooth forms can be represented by the conditional q -normal distribution function f_{CN} to describe this crossover. Moreover, the interpolating form of strength function given by f_{CN} is used to describe the fidelity decay after random k -body interaction quench and the formula for NPC valid in thermalization region is derived [25]. It is important to note that for bosonic systems, in addition to dilute limit (defined by $m \rightarrow \infty$, $N \rightarrow \infty$, and $m/N \rightarrow 0$), the dense limit (defined by $m \rightarrow \infty$, $N \rightarrow \infty$, and $m/N \rightarrow \infty$) is also feasible. For fermion systems, only dilute limit is possible. Therefore the focus was on the dense limit in the analysis of bosonic systems. Very recently, for fermionic EGOE($1+k$), the wave-function structure is analyzed by deriving the lower order moments of the strength functions in m -fermion spaces [48].

Going further, the purpose of the present study is to understand the mechanism of thermalization, in terms of the structure of chaotic eigenfunctions of isolated many-fermion systems, by varying the strength parameter λ of the k -body interaction in the EGOE($1+k$) Hamiltonian given by $H = h(1) + \lambda V(k)$, where $h(1)$ is one-body part of the interaction defined by single particle (sp) energies and $V(k)$ is the random k -body interaction. The focus is in the dilute limit as dense limit is not feasible for fermionic systems. The strength functions and measures based on them are basis dependent, we employ mean-field defined by fixed one-body part, as was done in the previous studies [25, 46, 48]. We utilize q -normal distribution f_N and conditional q -normal distribution f_{CN} to describe the smooth forms of state density as a function of λ and strength function in strong interaction domain, respec-

tively. The form of these functions can be completely determined by the parameters, the correlation coefficient ζ and q . A complete analytical description of ζ and q as a function of (m, N, k) are derived and they are tested with the ensemble averaged numerical results. Also, we analyze the lower moments of the so-called strength functions (also known as local density of states) by varying interaction strength λ and obtain a formula giving the critical strength $\lambda = \lambda_t$, in terms of model parameters m , N and k , for the onset of thermalization rather than choosing some specific value λ such that $\lambda \gg \lambda_t$ [46, 48]. Moreover, the region of thermalization is identified by comparing the moments of f_{CN} with that of the strength functions and shown that for $\lambda \geq \lambda_t$, the match between them is very good giving the region beyond which the strength functions follow f_{CN} . Further, the method of construction of strength functions is described so that their smooth forms can be correctly represented by f_{CN} . Results for inverse participation ratio are compared with smooth forms and found good agreement in the thermalization region.

The paper is organized as follows: The embedded ensembles EGOE(1+k) are briefly defined in Section II. Section III gives preliminary description about q -Hermite polynomials and conditional q -normal distributions. Results of state density along with a complete analytical description of the correlation coefficient ζ and q -parameter for fermionic EGOE(1+k) as a function of λ and body rank k are given in Section IV. In Section V A, the method of construction of strength functions is described for EGOE(1+k) giving Gaussian to semi-circle transition as body rank k increases from 2 to m in the strong interaction domain. More importantly, it is demonstrated that the conditional q -normal distribution function f_{CN} describes this transition correctly. Further, the first four moments of strength functions are studied and using the width of these strength functions, analytical formula for the chaos marker λ_t is derived in Section V B. Results for our calculations for IPR are presented in Section VI. Finally, Section VII gives the concluding remarks.

II. ENSEMBLES FOR FERMION SYSTEMS - EGOE(1+k)

Interactions between the constituents of finite isolated quantum systems, such as atomic nuclei, complex atoms and molecules, mesoscopic devices like small metallic grains and quantum dots, spin systems modeling a quantum computing core and so on, are known to be few-body in character. The random matrix ensembles (Gaussian orthogonal ensem-

bles (GOE)) which incorporate this feature along with nature of constituents (fermions, bosons, Majorana fermions and so on) are called embedded ensembles (Embedded Gaussian orthogonal Ensembles (EGOE)). Now we will briefly describe these ensembles for fermion systems.

Consider a system consisting of m spinless fermions occupying N sp states and interacting with each other via k -body ($k \leq m$) interactions. Distributing m such fermions in N degenerate sp states generates m -particle Hilbert space of dimension $d = \binom{N}{m}$. With sp states denoted by n_i , a basis state in k -particle space, in occupation number representation, is denoted by $|n_1 n_2 \cdots n_k\rangle$ with $\sum_{i=1}^k n_i = k$ and in increasing order, $n_1 < n_2 < \cdots < n_k$. m -particle basis states can be defined similarly. The k -body random Hamiltonian $V(k)$ for such a system in second quantization form can be defined as,

$$V(k) = \sum_{\alpha, \beta} w_{k; \alpha, \beta} F^\dagger(k; \alpha) F(k; \beta). \quad (1)$$

Here, α and β are the k -particle states in occupation number representation. $V(k)$ generates a k -particle Hilbert space of dimension $d_k = \binom{N}{k}$ with anti-symmetrized matrix elements $w_{k; \alpha, \beta}$ which are independent random variables. As the $V(k)$ matrix is chosen to be GOE in k -particle space, the k -particle matrix elements $w_{k; \alpha, \beta}$ are Gaussian random variables with zero mean and unit variance. The variance of diagonal matrix elements is $\overline{w_{k; \alpha, \alpha}^2} = 2$ while that of off-diagonal matrix elements, for ($\alpha \neq \beta$), is $\overline{w_{k; \alpha, \beta}^2} = 1$. Further, $F^\dagger(k; \alpha) = \prod_{i=1}^k f_{n_i}^\dagger$ and $F(k; \alpha) = (F^\dagger(k; \alpha))^\dagger$ with $F^\dagger(k; \alpha)$ (and $F(k; \alpha)$) are creation (and destruction) operators respectively for k -particle fermion state α . Similarly, $f_{n_i}^\dagger$ (and f_{n_i}) are the fermion creation (and destruction) operators respectively for sp state n_i . The action of this $V(k)$ on the m -particle basis states generates EGOE(k). Due to the k -body interactions, many of the matrix elements of the m -particle Hamiltonian matrix of EGOE(k) are zero for $m > k$ while many of the nonzero matrix elements are linear combinations of k -body matrix elements. This is different from what we have in the case of GOE. However when $k = m$, EGOE($k = m$) is identical to GOE by construction. Detailed study on these ensembles can be found out in [33] and references therein.

Now, adding the mean-field part generated by the presence of other fermions in the system, one can have EGOE($1 + k$) defined by,

$$H = h(1) + \lambda V(k) \quad (2)$$

Here, the mean-field given by the one-body operator $h(1) = \sum_{i=1}^N \varepsilon_i f_{n_i}^\dagger f_{n_i}$ is described by sp energies ε_i with average spacing Δ ; $f_{n_i}^\dagger f_{n_i}$ is the number operator for the i th sp state. Throughout this work, we use fixed sp energies $\varepsilon_i = i + 1/i$ to define $h(1)$, just as in many previous studies [25, 35, 36, 55]. Note that the second term $1/i$ in i has been added to avoid the degeneracy of many-particle states as discussed first in [36]. The parameter λ represents k -body interaction strength. With $\Delta = 1$, λ is measured in units of the average spacing of the sp energies defining $h(1)$.

In the present study, we utilize q -normal distribution f_N and conditional distribution f_{CN} and the results are presented for the onset of thermalization in these systems using the lower order moments of the strength functions. The numerical results are obtained by fully diagonalizing EGOE(1+ k) ensemble for various values of body rank k and interaction strength λ . The following two examples of EGOE(1+ k) are considered: (i) 100 member ensemble with $m = 6$ fermions in $N = 12$ sp states and dimensionality of system is $d = 924$; (ii) 20 member ensemble with $m = 7$ fermions in $N = 14$ sp states and dimensionality of the system is $d = 3432$. The ensemble average is carried out by making the spectra of each member of the ensemble zero centered and scaled to unit width.

III. q -HERMITE POLYNOMIALS AND CONDITIONAL q -NORMAL DISTRIBUTION

L. J. Rogers first introduced q -Hermite polynomials in Mathematics to prove the Rogers–Ramanujan identities [56] and their important properties are due to Szego and Carlitz [57]. The q -Hermite polynomials are related with the Chebyshev, Rogers-Szego, Al-Salam-Chihara polynomials and others. Recently they have found applications in non-commutative probability, quantum physics, combinatorics and so on. Also the q -calculus has attracted many researchers working in the field of special functions as it is a very powerful tool in quantum computation [58].

Let us begin with q -numbers, $[n]_q = (1 - q)^{-1}(1 - q^n)$ and q -factorials, $[n]_q! = \prod_{j=1}^n [j]_q$, which define the q -Hermite polynomials. We have $[n]_{q \rightarrow 1} = n$. Also, $[0]_q! = 1$. The recursion relation that defines the q -Hermite polynomials $\mathbf{H}_n(x|q)$ is given as [56],

$$x \mathbf{H}_n(x|q) = \mathbf{H}_{n+1}(x|q) + [n]_q \mathbf{H}_{n-1}(x|q). \quad (3)$$

Here, $\mathbf{H}_0(x|q) = 1$ and $\mathbf{H}_{-1}(x|q) = 0$. The q -Hermite polynomials with $q = 1$ give normal Hermite polynomials, which are related to Gaussian and with $q = 0$ give Chebyshev polynomials, which are related to semi-circle. Importantly, the weight function of q -Hermite polynomials is the q -normal distribution $f_N(x|q)$ defined by [47],

$$f_N(x|q) = \frac{1}{2\pi} \sqrt{\frac{1-q}{4-(1-q)x^2}} \prod_{i=0}^{\infty} [(1+q^i)^2 - (1-q)q^i x^2] (1-q^{i+1}). \quad (4)$$

q -Hermite polynomials are orthogonal within the limits $s(q) = [-2/\sqrt{1-q}, 2/\sqrt{1-q}]$, which can be inferred from the following property,

$$\int_{s(q)} dx \mathbf{H}_n(x|q) \mathbf{H}_m(x|q) f_N(x|q) = [n]_q! \delta_{mn}. \quad (5)$$

Here, x is normalized variable, with zero centroid and unit variance, and $-2/\sqrt{1-q} \leq x \leq 2/\sqrt{1-q}$. In general q can take any value from $[-1,1]$, however in the present study $q \in [0,1]$. Note that $\int_{s(q)} dx f_N(x|q) = 1$ and one can see that in the limit $q \rightarrow 1$, $f_N(x|q)$ will take Gaussian form and in the limit $q \rightarrow 0$, $f_N(x|q)$ will take semi-circle form.

Further, the bivariate q -normal distribution $f_{biv-qN}(x, y|\zeta, q)$ with standardized variables x and y is defined as [47, 54],

$$f_{biv-qN}(x, y|\zeta, q) = f_N(x|q) f_{CN}(y|x; \zeta, q) = f_N(y|q) f_{CN}(x|y; \zeta, q). \quad (6)$$

Here ζ is the bivariate correlation coefficient. $f_N(x|q)$ and $f_N(y|q)$ are the marginal densities of $f_{biv-qN}(x, y|\zeta, q)$. Then, the conditional q -normal densities, f_{CN} can be given as,

$$f_{CN}(x|y; \zeta, q) = f_N(x|q) v(x, y|\zeta, q);$$

$$f_{CN}(y|x; \zeta, q) = f_N(y|q) v(x, y|\zeta, q);$$

$$v(x, y|\zeta, q) = \prod_{i=0}^{\infty} \frac{(1 - \zeta^2 q^i)}{(1 - \zeta^2 q^{2i})^2 - (1 - q)\zeta q^i(1 + \zeta^2 q^{2i})xy + (1 - q)\zeta^2(x^2 + y^2)q^{2i}}. \quad (7)$$

Also,

$$\int_{s(q)} dx \mathbf{H}_n(x|q) f_{CN}(x|y; \zeta, q) = \zeta^n \mathbf{H}_n(y|q). \quad (8)$$

From the above relation, it is clear that f_{CN} and f_{biv-qN} are normalized to 1 over the range $s(q)$.

Recently, it has been shown that the smooth forms of eigenvalue density and strength functions for embedded ensembles with k -body interactions, EGOE(k), can be described f_N (equation 4) [29, 46] and by f_{CN} (equation 7) [25] respectively giving transition from Gaussian form to semi-circle form as k changes from 2 to m . Going beyond this, we will show in the next section that f_N can also describe the shape of the state density (intermediate form between Gaussian to semi-circle) as the interaction λ increases in fermionic EGOE($1+k$) just like bosonic systems [25]. Also, given is a complete analytical description of variation of correlation coefficient ζ and parameter q with λ .

IV. STATE DENSITY AND FORMULA OF CORRELATION COEFFICIENT ζ AND PARAMETER q FOR EGOE($1+k$)

A. State density

In figure 1 histograms represent ensemble averaged state density vs. normalized energy for EGOE($1+k$) examples for various values of k and for different interaction strength λ . Results are shown for EGOE($1+k$) ensemble with $m = 6$ fermions occupying $N = 12$ sp states (figure 1(a)) and with $m = 7$ fermions occupying $N = 14$ sp states (figure 1(b)). The sp energies defining the one body Hamiltonian $h(1)$ are chosen to be $\varepsilon_i = i + 1/i$, $i = 1, 2, \dots, N$. In the calculation, firstly the spectra of each member of ensemble is zero centered (with centroid ϵ_H) and scaled to unit width (with width σ_H) and then ensemble averaged histograms are obtained. The smooth red curves in figure 1 are obtained using equation 4 and are given as,

$$\rho(E) dE = dE \frac{\mathcal{N}}{\sigma_H} \sqrt{\frac{1-q}{1 - \left(\frac{E-\epsilon_H}{E_0}\right)^2}} \times \prod_{i=0}^{\infty} (1 - q^{i+1}) \left[(1 + q^i)^2 - q^i 4 \left(\frac{E - \epsilon_H}{E_0}\right)^2 \right]; \quad (9)$$

$$E_0^2 = \frac{4\sigma_H^2}{1-q}, \quad \epsilon_H - \frac{2\sigma_H}{\sqrt{1-q}} \leq E \leq \epsilon_H + \frac{2\sigma_H}{\sqrt{1-q}}.$$

Here, \mathcal{N} is the normalization factor and ensemble averaged values of parameter q are also given in the figure. As the tails of the distribution are an important aspect from a random matrix theory point of view, semi-log scale is used in figure 1 in order to see the comparison

between the tails of the histograms with the analytical prediction given by equation 9. The results clearly show that with small deviations near tails, the q -normal distribution f_N correctly describes the intermediate form (i.e. between Gaussian to semi-circle) for the state density as λ and k changes in EGOE(1+k).

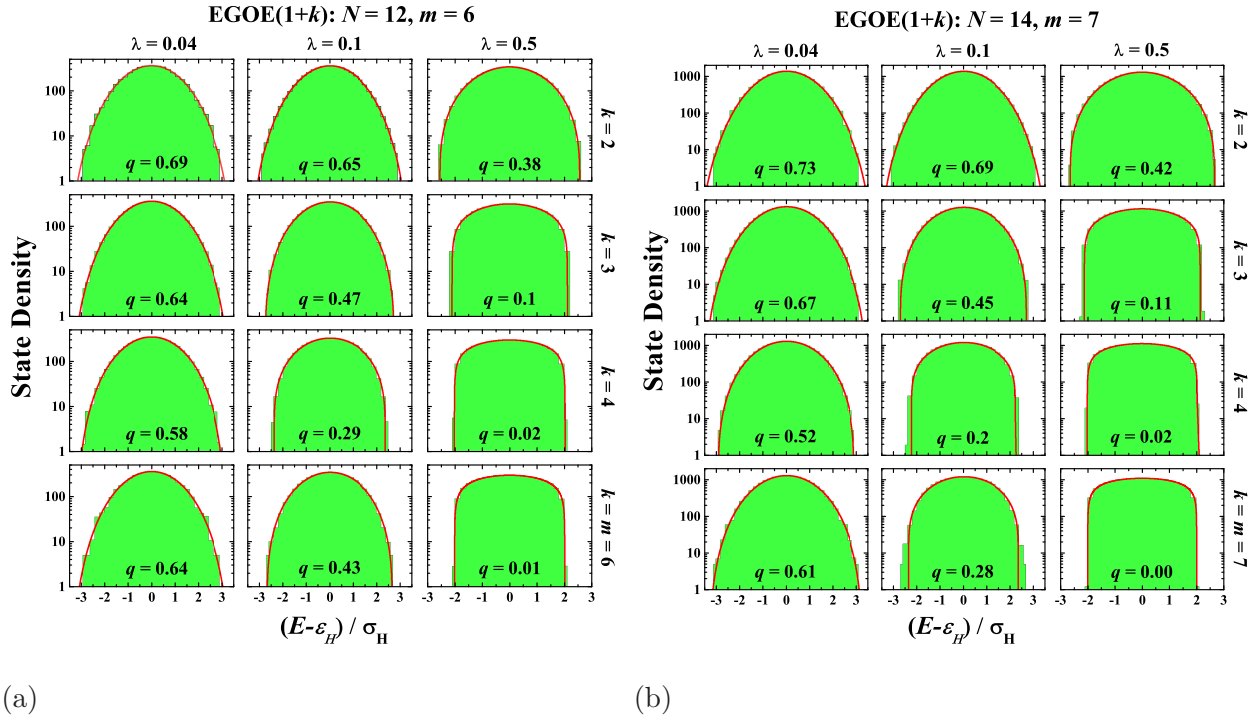


FIG. 1. Ensemble averaged state density $\rho(E)$ vs. normalized energy E results for EGOE(1 + k) examples (a) a 100 member ensemble with $m = 6$ fermions in $N = 12$ sp states and (b) a 20 member ensemble with $m = 7$ fermions in $N = 14$ sp states. Results are shown for different values of interaction strength $\lambda = 0.04, 0.1, \text{ and } 0.5$ for $k = 2, 3, 4$ and $k = m$. Ensemble averaged state density histograms are compared with $\rho(E)$ given by equation 9 (red smooth curves) with the corresponding ensemble averaged q values given in each panel. In all the plots $\int dE \rho(E) = d$.

B. Correlation coefficient ζ and its variation with λ

The correlation coefficient ζ between $h(1)$ and full Hamiltonian H is defined as

$$\zeta = \sqrt{\frac{\sigma_{h(1)}^2}{\sigma_{h(1)}^2 + \lambda^2 \sigma_{V(k)}^2}}.$$

ζ is also related to the width of the strength functions; see section VB2 ahead for further details. The analytical expression of ζ in terms of model parameters for fermionic EGOE(1+k) can be derived as follows: For $H = V(k)$ i.e. with all sp energies as degenerate, we have [33],

$$\sigma_{V(k)}^2 = P(N, m, k) \binom{N}{k}^{-1} \sum_{\alpha, \beta} \overline{w_{k; \alpha, \beta}^2}, \quad (10)$$

$$\text{where } P(N, m, k) = \binom{N}{k}^{-1} \Lambda^0(N, m, k).$$

Here, α and β denote k -particle states. As the $V(k)$ matrix is GOE in k -particle space, for EGOE(k), we have

$$\sigma_{V(k)}^2 = P(N, m, k) \left\{ \binom{N}{k} + 1 \right\}. \quad (11)$$

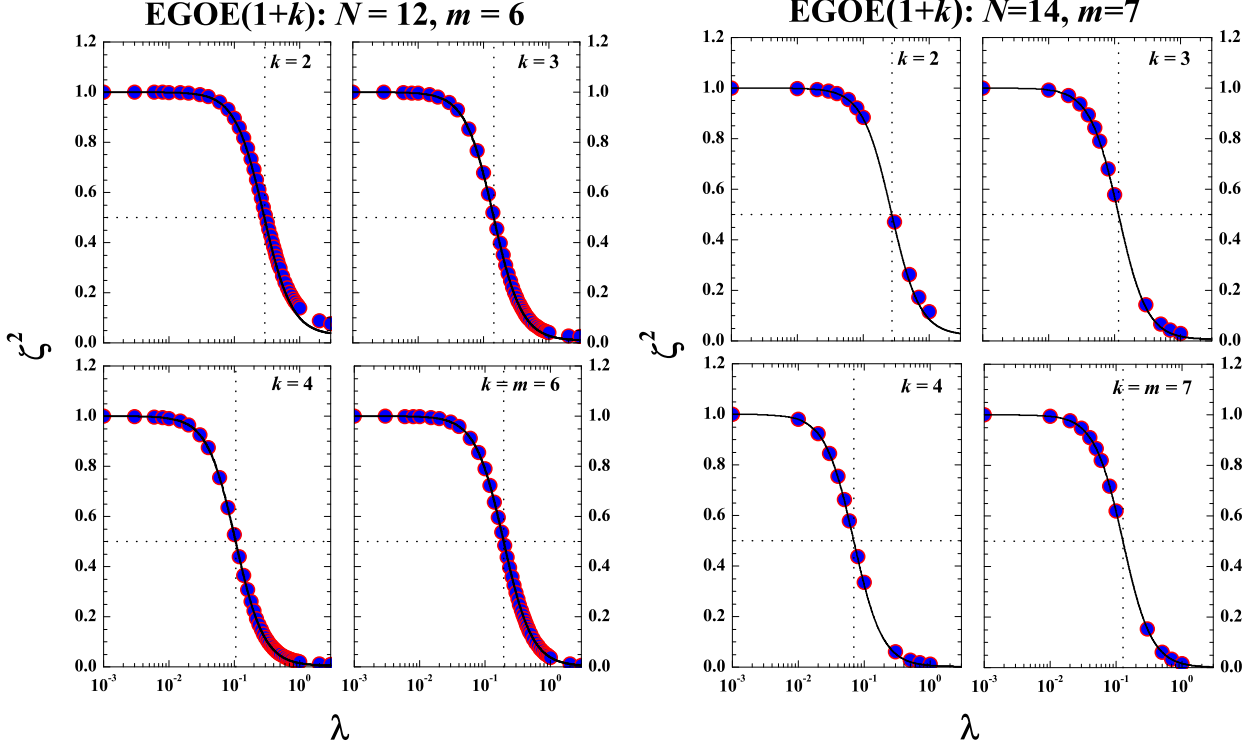
For one body $h(1)$ part of the Hamiltonian defined by the external sp energies ε_i we have,

$$\sigma_{h(1)}^2 = \frac{m(N-m)}{N(N-1)} X. \quad (12)$$

Here, $X = \sum \tilde{\varepsilon}_i^2$; $\tilde{\varepsilon}_i$ are the trace-less sp energies of i 'th state. With inclusion of the contribution from the diagonal part of $V(k)$, the analytical expression for ζ^2 can be given by,

$$\zeta^2 = \frac{\frac{m(N-m)}{N(N-1)} X + 2 \lambda^2 P(N, m, k)}{\frac{m(N-m)}{N(N-1)} X + \lambda^2 P(N, m, k) \left\{ 1 + \binom{N}{k} \right\}}. \quad (13)$$

Now we test equation 13 with numerical ensemble averaged EGOE(1+k) results. We consider two examples for this analysis: (i) a 100 member EGOE(1+k) ensemble with $m = 6$ fermions in $N = 12$ sp states and (ii) a 20 member EGOE(1+k) ensemble with $m = 7$ fermions in $N = 14$ sp states. The variation of ζ^2 as a function of λ is obtained for various values of the body rank k for both these examples and results are presented in figure 2. In all these plots the solid circles represent the numerical ensemble averaged results while the black smooth curves are due to analytical results obtained using equation 13. It is clear from the figure that ζ^2 is close to 1 for smaller λ and as λ increases, ζ^2 goes on decreasing smoothly and approaches 0 for all body rank k . The numerical results are in very good agreement with the analytical expression given by equation 13 for all k values for both the examples. Small discrepancy is due to neglect of induced sp energies given by $V(k)$ for smaller k . With increasing k , contribution of the induced sp energies will steadily tend to reduce, while that of external sp energies remain fixed.



(a)

(b)

FIG. 2. Ensemble averaged ζ^2 (solid circles) as a function of interaction strength λ for (a) 100 member EGOE(1+k) ensemble with $m = 6$ and $N = 12$ and (b) 20 member EGOE(1+k) ensemble with $m = 7$ and $N = 14$ for $k = 2, 3, 4$ and $k = m$. The ensemble averaged results are compared with the analytical curves given by equation 13 (smooth black curves). A very good agreement between ensemble averaged results and analytical formula, given by equation 13, can be seen for both the examples. The vertical dotted line, in each panel, corresponds to λ_t (defined ahead in section VB2), obtained with the condition $\zeta^2 = 0.5$, giving thermodynamic region. See text for further details.

C. Variation of parameter q with λ

From the results shown in figure 1, the ensemble averaged state density takes intermediate form between Gaussian to semi-circle as λ and k change in EGOE(1+k) and the univariate q -normal distribution f_N can describe this transition correctly. With $\lambda = 0$, the formula of

q for one-body part $h(1)$ only, using trace propagation formula is given by,

$$\begin{aligned}
q_h + 2 &= \langle h(1)^4 \rangle^m \\
&= \frac{3(m-1)N(N-1)(N-m-1)}{m(N-2)(N-3)(N-m)} + \frac{N(N-1)[N^2 + N - 6mN + 6m^2]}{m(N-m)(N-2)(N-3)} \frac{Y}{X^2}
\end{aligned} \tag{14}$$

Here, $\langle h(1)^4 \rangle^m$ is the reduced fourth moment of $h(1)$ and $Y = \sum \tilde{\varepsilon}_i^4$. Figure 3 represents variation of q_h as a function of m fermions. The results are shown for various values of m/N using equation 14 with fixed sp energies employed in the present study. From the results, one can see that q_h varies from close to zero to 1 as m increases from body rank $k = 1$ to higher values. This is due to fact that the form of the eigenvalue density for a m particle system with k -body interactions is semi-circle for $k = m$ and Gaussian for $k \ll m$ [50, 51]. In the dilute limit, with $m \rightarrow \infty, N \rightarrow \infty, m/N \rightarrow 0$, the first term in equation 14 reduces to 3 and the second term vanishes and q_h approaches to 1. The smooth curve in figure 3 corresponds to dilute limit. Going further, formula of q parameter for complete Hamiltonian $H = h(1) + \lambda V(k)$ for fermionic systems i.e. for EGOE(1+k) can be given by [48],

$$\begin{aligned}
q_H + 2 &= \frac{\langle h(1) + \lambda V(k) \rangle^m}{\sigma_H^4}, \\
q_H &= \zeta^4 q_h + 2\zeta^2 (1 - \zeta^2) q_{hV} + (1 - \zeta^2)^2 q_V.
\end{aligned} \tag{15}$$

Here, q_V represents parameter q for random k -body interaction $H = V(k)$, with all sp energies as degenerate. The formula for q_V in terms of N, m and k can be given as [46],

$$q_V = \frac{\sum_{\mu=0}^{\min(k, m-k)} \Lambda^\mu(N, m, k) \Lambda^\mu(N, m, m-k) d(N : \mu)}{\binom{N}{m} [\Lambda^0(N, m, k)]^2}, \tag{16}$$

$$\Lambda^\mu(N, m, r) = \binom{m-\mu}{r} \binom{N-m+r-\mu}{r}, \quad d(N : \mu) = \binom{N}{\mu}^2 - \binom{N}{\mu-1}^2.$$

Similarly, q_{hV} can be written as,

$$q_{hV} = \frac{\sum_{\mu=0}^{\min(1, m-k)} \Lambda^\mu(N, m, k) \Lambda^\mu(N, m, m-1) d(N : \mu)}{\binom{N}{m} \Lambda^0(N, m, 1) \Lambda^0(N, m, k)}. \tag{17}$$

Figure 4 shows the results of complete variation of q_H as the strength of k -body interaction λ increases in EGOE(1+k). The ζ values are obtained using equation 13. The formula given by equations 15 is tested using the two examples considered in the present analysis:

(i) a 100 member EGOE(1+k) ensemble with ($m = 6, N = 12$) and (ii) a 20 member EGOE(1+k) ensemble with ($m = 7, N = 14$). For these systems, with given λ and body rank k , we construct EGOE(1+k) ensemble and q_H is computed using the eigenvalues. The solid symbols in figure 4 represent ensemble averaged values, while the vertical bars are corresponding widths of the distributions of q_H computed over members of ensemble. The continuous curves are obtained via equations 13-17. The agreement between the ensemble averaged results and analytical expression is good for smaller values of λ and $k > 2$. The deviations between numerics and smooth forms for stronger interaction strength λ with smaller k are due to following reasons:(i) neglected the contribution of induced sp energies in the computation of ζ (see section IV B for further details); (ii) The formula for q_{hV} , given in equation 17, is valid for random sp energies while in the numerical results are for fixed sp energies. In the figure 4 the horizontal marks on the left correspond to value of parameter q_h and those on the right correspond to q_V . One can observe that when the value of λ is very small, the ensemble averaged values of q_H are found very close to q_h given by equation 14. Now we gradually increase λ and for a sufficiently large value, the ensemble averaged q_H values approach the corresponding q_V values. The formula given by equation 15 gives good description of q as k -body interaction strength λ varies in EGOE(1+k). Also, from the results shown in figure 4, one can see that for a fixed k , the state density takes intermediate form between Gaussian to semi-circle as λ changes in EGOE(1+k) and the transition in state density can be described using f_N formula with values of parameter q_H given by equation 15.

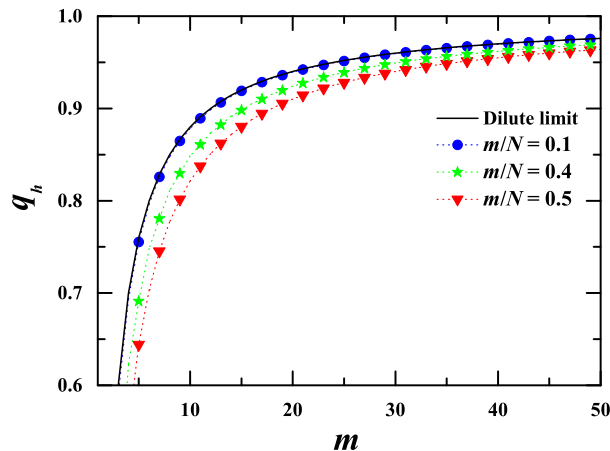
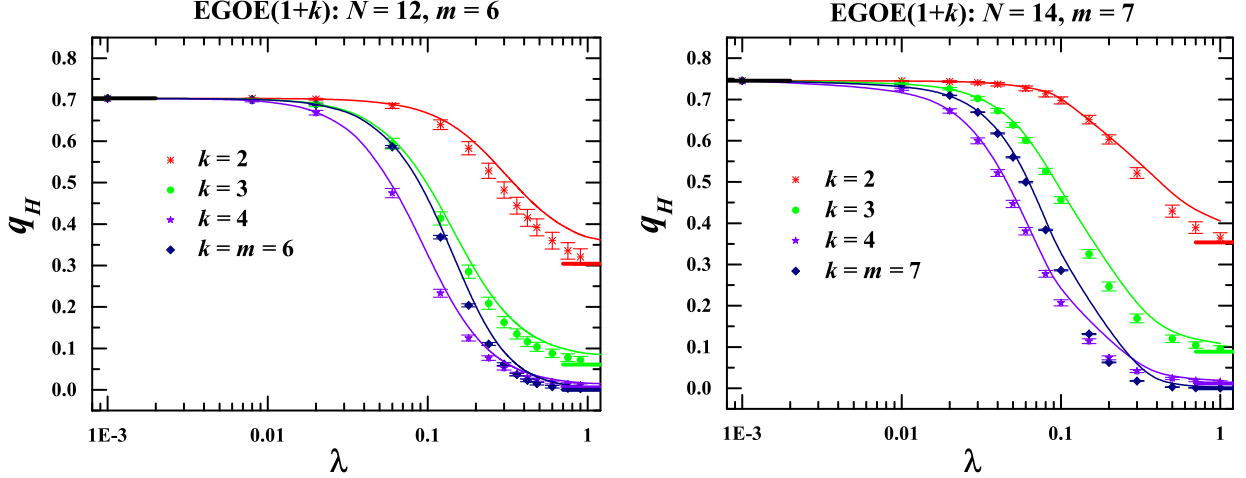


FIG. 3. Variation of q_h as a function of number of fermions for different m/N values.



(a) (b)

FIG. 4. Variation of ensemble averaged q vs. λ for EGOE(1+k) ensemble for system of (a) 100 member EGOE(1+k) with $m = 6$ fermions in $N = 12$ sp states and (b) 20 member EGOE(1+k) with $m = 7$ fermions in $N = 14$ sp states. Results are shown for $k = 2, 3, 4$ and $k = m$. The widths of distribution of q_H are shown by vertical bars.

V. STRENGTH FUNCTIONS

A. Definition and results for EGOE(1+k)

The statistical properties related to the structure of wavefunction can be studied via so called strength functions as they carry all of the information about wavefunction structure. Since strength functions are experimentally measurable quantities they are of great importance [10]. Here, we will study strength functions to understand the structure of eigenfunctions of EGOE(1+k) expanded in terms of $h(1)$ basis states. Given set of basis states $|\phi_\kappa\rangle$ for m -fermions distributed in N sp states, the diagonal matrix elements of $H(m)$ are denoted as $\xi_\kappa = \langle \phi_\kappa | H | \phi_\kappa \rangle$. Diagonalization of the full Hamiltonian H gives eigenenergy E_i and corresponding eigenfunction $|\psi_i\rangle$; $H |\psi_i\rangle = E_i |\psi_i\rangle$. The eigenstates $|\psi_i\rangle$ are related to m -particle basis states $|\phi_\kappa\rangle$ as $|\phi_\kappa\rangle = \sum_{i=1}^d C_\kappa^i |\psi_i\rangle$. Here d is the dimensionality of m -fermion space and C_κ^i denotes expansion coefficients of the basis state $|\phi_\kappa\rangle$ in terms of the eigenstates $|\psi_i\rangle$. With this we can define the strength function corresponding to a particular basis state $|\phi_\kappa\rangle$ as

$$F_{\xi_\kappa}(E) = \sum_i |C_\kappa^i|^2 \delta(E - E_i) = \overline{|C_\kappa^E|^2} I(E), \quad (18)$$

where $I(E)$ is the state density and $\overline{|C_\kappa^E|^2} = \frac{1}{I(E)} \sum_{E_i \in E} |C_\kappa^i|^2$. The definition takes into account the degeneracy in the eigen spectrum; Note that the last relation in equation 18 is valid only when the average is supported by chaos, not in general.

It is well known that for $H = h(1)$, strength functions are delta functions as the basis state $|\phi_\kappa\rangle$ are identical to eigenstates $|\psi_i\rangle$. With interaction switched on in EGOE(1+k), the basis state $|\phi_\kappa\rangle$ spreads into the eigenstates $|\psi_i\rangle$ and the strength functions take the Breit–Wigner (BW) form. With further sufficient increase in $\lambda > \lambda_t$, the BW form changes to f_{CN} form and ensemble averaged strength functions of many-body interacting particle systems with k -body interaction can be represented by smooth forms given by f_{CN} [25, 48].

In order to compute the ensemble averaged strength function $F_\xi(E)$ in EGOE(1+k), with λ sufficiently large where f_{CN} form is applicable, we adopted the procedure used in [25]. In the ensemble averaged calculations, the E_i and ξ_κ spectra are scaled to have zero centroid and unit width for each member of the ensemble using the eigenvalue distribution and κ -energies distribution, respectively. Therefore, $E \rightarrow \hat{E}$ and $\xi/\sigma_H = \zeta \hat{\xi}$. Now, with this scaling the method of construction of strength function used in the previous studies can apply [25, 55, 59]. Figure 5 shows the ensemble averaged strength function results obtained for two EGOE(1 + k) examples with (i) $m = 6$ fermions in $N = 12$ sp states and (ii) $m = 7$ fermions in $N = 14$ sp states. Here λ is chosen equal to 0.5, so that the system is in thermalization region [46]. The ensemble averaged $F_\xi(E)$ results are shown for $\hat{\xi} = 0.0, \pm 0.5, \pm 1.0, \pm 1.5$ and ± 2.0 using body rank $k = 2, 3, 4$ and m for both the examples. All these strength function histograms $F_\xi(E)$ are fitted with $f_{CN}(\hat{E}|\hat{\xi}; \zeta, q = q_H)$. For each k , the smooth curves in figure 5 are obtained with f_{CN} using corresponding ensemble averaged values of ζ and q_H . It is clearly seen from the results shown in the figure that the ensemble averaged histograms are in very good agreement with the smooth forms obtained using f_{CN} . The vertical dotted lines in each panel of figure 5, represent the centroid ε_F and it is equal to $\zeta \xi$. Following conclusions can be derived from the results shown in the figure 5: (i) One clearly sees that for sufficiently large λ , the smooth part of strength functions $F_\xi(E)$ are very well represented by f_{CN} and they make a transition from Gaussian form to semi-circle form, as the body rank k in EGOE(1+k) changes from 2 to m . (ii) $F_\xi(E)$ results for $\hat{\xi} = 0$ are symmetric (extreme left panels in figure 5). (iii) Now for $\hat{\xi} \neq 0$, away from the center of the spectrum, $F_\xi(E)$ results are asymmetrical about \hat{E} as demonstrated earlier [25, 55]. (iv) The centroid of $F_\xi(E)$ changes with k for $\hat{\xi} \neq 0$. (v) $F_\xi(E)$ are more skewed in the positive

direction for negative $\hat{\xi}$ values and are more skewed in the negative direction for positive $\hat{\xi}$ values. From these results and also obtained in [25, 48], one can clearly conclude that the strength functions of many-particle systems with random k -body interactions, follow the conditional q -normal distribution f_{CN} . It is important to note that for $\lambda = 0$, i.e. with one-body interaction alone, the basis states themselves are the eigenstates and hence $F_{\xi}(E)$ then corresponds to the δ function for all k . With increase in λ , the shape of $F_{\xi}(E)$ changes from the Breit-Wigner (BW) form. With further increase in λ , the shape of $F_{\xi}(E)$ changes to Gaussian or semi-circle or intermediate to Gaussian and semi-circle depending upon the values of λ and k . Therefore, one can also observe the BW to Gaussian to semi-circle transition in $F_{\xi}(E)$ by changing both λ and k . The f_{CN} can not give BW form for $F_{\xi}(E)$ in any limit and it is possible to study BW to semi-circle transition in $F_{\xi}(E)$ using hybrid expression given in [60].

Very recently, it is shown that for EGOE(1+k) with sufficiently large λ , the first four moments of $F_{\xi}(E)$ are very close to that of f_{CN} , analytically [48] as well as numerically [25]. In the next section, we will further analyze strength functions of EGOE(1+k) by computing their first four moments and to identify the region of thermalization by comparing them with corresponding smooth expressions given by f_{CN} .

B. Lower order moments of Strength functions

1. Centroid ε_F

From the results of previous section, it is clear that asymmetry in strength function with respect to \hat{E} and $\hat{\xi}$ increases and also the centroid of the strength function moves with $\hat{\xi}$. The centroid of f_{CN} is given by $\varepsilon_F = \zeta \hat{\xi}$ and it is compared with the ensemble averaged centroid of $F_{\kappa}(E)$ computed for a 100 member EGOE(1+k) with $(m, N) = (6, 12)$. Figure 6 represents the variation of ε_F with λ for $k = 2$ and 3. The ensemble averaged results (symbols) are compared with expression given by f_{CN} (smooth curves) and the match between them is exact. From the results, it is clear that the peak values of $F_{\kappa}(E)$ change with $\hat{\xi}$ and the rate of change of ε_F with respect to $\hat{\xi}$ is given equal to the correlation coefficient ζ .

2. Width σ_F and thermalization marker λ_t

The expression for the normalized width of the strength functions σ_F is exactly same as that of f_{CN} and it is $\sigma_F = \sqrt{1 - \zeta^2}$. The width σ_F (independent of ξ) of the strength functions is scaled by the spectrum width σ_H and ζ is the correlation coefficient which determines the thermodynamic chaos marker [25]. Therefore, the variation of σ_F can be discussed in terms of ζ^2 results given in Section IV B. The thermodynamic region is the region where different quantities defining the eigenstate properties like entropy, strength functions, temperature, etc. give the same values irrespective of the defining basis. This means that once the interaction strength λ between the particles goes beyond λ_t , the quantum system thermalizes and then we can define quantities like temperature, entropy, etc. of the system. Very recently, analytical expression of λ_t is obtained for interacting dense boson systems in [25]. The critical value of the interaction strength is obtained extending the concept of duality to EGOE(1+k). As first discussed in [61], at duality point $\lambda = \lambda_t$, the quantities defining eigenstate properties like strength functions, entropies, temperature, etc. give the same values irrespective of the defining basis. With $H = h(1) + \lambda V(k)$, we have two choices of basis: one defined by one-body h and other by infinite interaction V . The variance of one-body part can be given as $\sigma_h^2 = a^2 \Delta^2$ and that of interaction part $\sigma_V^2 = b^2 \lambda^2$. Now, for the strength functions expanded in one-body basis, the correlation coefficient is by $\zeta_h = \sqrt{a^2 \Delta^2 / (a^2 \Delta^2 + b^2 \lambda^2)}$. Similarly, for the strength functions expanded in interaction basis, the correlation coefficient is by $\zeta_V = \sqrt{b^2 \lambda^2 / (a^2 \Delta^2 + b^2 \lambda^2)}$. At duality point $\lambda = \lambda_t$, it can be seen that the spreading produced by one-body part and k -body part are equal ($\zeta_V = \zeta_h$) giving condition that $\zeta^2 = 0.5$ [62]. Putting $\zeta^2 = 0.5$ in equation 13 and solving it for λ , (m, N, k) dependence of marker λ_t is obtained as,

$$\lambda_t = \sqrt{\frac{m(N-m) X}{N(N-1)\Lambda^0(N, m, k)(1 - 3 \binom{N}{k}^{-1})}}. \quad (19)$$

Using above equation, we have $\lambda_t(k=2) = 0.2944$, $\lambda_t(k=3) = 0.1448$ and $\lambda_t(k=4) = 0.1053$ for $m=6, N=12$). Similarly, with $(m=7, N=14)$, $\lambda_t(k=2) = 0.2764$, $\lambda_t(k=3) = 0.1158$ and $\lambda_t(k=4) = 0.0696$. λ_t results for $k=2$ are consistent with theoretical estimates obtained in [62]. The results of the variation of marker λ_t (which defines the thermodynamic region) as a function of m are presented in figure 7. Results are shown for m/N values 0.1 and 0.5 for $k=2, 3$ and 4. It can be clearly seen that value

of λ_t decreases as the body rank of interaction k among the particles increases i.e. the thermalization sets in faster in the system with increase in rank of interaction k . Further, in the results of ζ^2 given in figure 2, the vertical dash-lines indicate the positions of λ_t for given k obtained using equation 19. It can be clearly seen that $\zeta^2 = 0.5$ gives the thermalization point λ_t correctly for given body rank of the interaction k .

Now in the next section, we will analyze the ensemble averaged results of skewness γ_1 and excess γ_2 of $F_\xi(E)$ as a function of λ with that of f_{CN} and show that they can be used to identify the thermodynamic region λ_t .

3. Skewness γ_1 and Excess γ_2

The simple analytical expressions for γ_1 and γ_2 of f_{CN} can be given as [48],

$$\begin{aligned}\gamma_1(\hat{\xi}) &= -\frac{\varepsilon_F(1-q)}{\sigma_F}, \\ \gamma_2(\hat{\xi}) &= (q-1) + \gamma_1^2 \left(1 + \frac{(1+q)}{(1-q)\hat{\xi}^2}\right),\end{aligned}\tag{20}$$

We have computed ensemble averaged γ_1 and γ_2 of $F_\xi(E)$ for a 100 member EGOE(1+k) with $m = 6$ fermions in $N = 12$ sp states as a function of λ , for body rank of interaction $k = 2$ and 3, and the results are shown in figure 8 for various values of $\hat{\xi} = 0, \pm 1.0, \pm 2.0$. The solid symbols represent EGOE(1+k) results while the smooth forms are obtained using the formulas given in equation 20. From the results shown in the figure, it is clear that γ_1 is non zero for $\hat{\xi} \neq 0$, γ_1 is positive for $\hat{\xi} < 0$ and negative for $\hat{\xi} > 0$. This feature is clearly visible in the strength function results presented in previous section. Further, γ_2 is always positive for $\pm\hat{\xi}$. In the thermodynamic region with $\zeta^2 \leq 0.5$, $\gamma_2 \approx (q-1)$ as suggested in [25]. For smaller value of λ , the deviation between numerical results and the corresponding smooth forms of γ_1 and γ_2 , are very large indicating f_{CN} forms can not be applied to represent strength functions $F_\xi(E)$ at this stage. Further, for sufficiently large $\lambda(\geq \lambda_t)$ where f_{CN} form is applicable to $F_\xi(E)$, the deviation between ensemble averaged results and smooth forms for γ_1 and γ_2 decreases to zero giving onset of thermalization marker λ_t . In figure 8, λ_t is shown by vertical dotted lines for each k results. The λ_t values obtained from moments are in good agreement with those obtained from analytical results using equation 19. Hence, the onset of thermalization in quantum many-fermion systems with k -body interactions can also be located using the moments of $F_\xi(E)$.

VI. INVERSE PARTICIPATION RATIO (IPR)

IPR (also known as NPC) is a useful quantity to measure the degree of delocalization of a given eigenstate within a specific basis. It gives essentially the number of basis states $|\phi_\kappa\rangle$ that make up the eigenstate $|\psi_i\rangle$ with energy E . For an eigenstate $|\psi_i\rangle$ spread over the basis states $|\phi_\kappa\rangle$, with energies $\xi_\kappa = \langle\phi_\kappa|H|\phi_\kappa\rangle$, it is defined as,

$$\text{IPR}(E) = \left\{ \sum_{\kappa} |C_{\kappa}^i|^4 \right\}^{-1}. \quad (21)$$

For the case of full localization, the $|\psi_i\rangle$ state is one of the basis states, so only one $C_{\kappa}^i = 1$ giving IPR close to 1. On the other hand, if the state $|\psi_i\rangle$ is equally distributed among all basis states giving GOE value of $\text{IPR} = d/3$ with d is the dimensionality of the m -particle space. Recently, a simple two-parameter expression for $\text{IPR}(E)$, applicable to one-body plus an embedded GOE of k -body interaction for interacting many-particle systems, is derived in [25]. This expression is valid in the chaotic domain ($\lambda \leq \lambda_t$) where the level fluctuations follow GOE [49] and the form of the strength functions is very well represented by f_{CN} . This expression for $\text{IPR}(E)$ is given as,

$$\text{IPR}^{\zeta,q}(E) = \frac{d}{3} \left\{ \sum_{n=0}^{\infty} \frac{\zeta^{2n}}{[n]_q!} [\mathbf{H}_n(\hat{E}|q)]^2 \right\}^{-1}, \quad (22)$$

The parameters ζ and q are described in sections IV B and IV C, respectively. The equation 22 can be applicable to fermionic EGOE(1+k) as it depends only on the parameters, ζ and q , defining the shape of f_N and f_{CN} . The equation 22 is tested with ensemble averaged EGOE(1+k) results for fermion systems for various values of k . Ensemble averaged IPR results are presented in figure 9, by considering a 100 member EGOE(1+k) ensemble with $m = 6$ fermions in $N = 12$ sp states example for different values of λ for body rank $k = 2, 3, 4$ and $k = m = 6$. The blue solid circles represent the ensemble averaged IPR values. The smooth curves are due to the theoretical expression given by equation 22 and the ensemble averaged ζ and q values used for this analysis are given in the corresponding figures. One can clearly see the localization to delocalization transition with increase in λ for fixed k from these results. When the value of λ is very small, i.e. when the one-body part of the interaction dominates over the k -body interaction, the IPR values are close to one and a large deviation between the numerical results and the theoretical curves is observed. This indicates the wavefunctions are completely localized in this region. Now as λ is

slightly increased, the deviation between the numerical results and the theoretical curves is still observed, however it is reduced compared to the previous case as the chaos has not yet set in the system. Now when λ is increased to a sufficiently high value ($\lambda = \lambda_t$), one can see that in the bulk of the spectrum there is a good match between ensemble averaged results and theoretical curves whereas small deviations are observed near the spectrum tails. In this region the system is in chaotic domain corresponding to the thermalization region given by $\zeta^2 \sim 1/2$ [31] and the smooth variation of strength functions $F_\xi(E)$ are well represented by f_{CN} and IPR reaches the theoretical chaotic domain estimate value for all k . It can be clearly seen from the results that for $\lambda \geq \lambda_t$, the match of the theoretical expression and the ensemble averaged numerical results, is very good for all k ; indicating onset of thermalization and the wavefunctions are delocalized in this region.

VII. CONCLUSIONS

In the present paper, we have studied the conditions of thermalization in fermion systems with EGOE(1+k) using the measures based on the structure of eigenfunctions, the shape of strength functions and IPR, as a function of the interaction strength λ and for various values of body rank of the interaction k . It is shown that q -normal distribution f_N defining q -Hermite polynomials can describe the smooth part of the state density in interacting fermion systems in dilute limit just like their bosonic counter part in dense limit [25]. An analytical expression is derived for the q_h -parameter for fixed one body part $h(1)$ and it is shown that in the dilute limit $q_h \rightarrow 1$. Also a complete description of q_H -parameter is obtained as a function of the strength of interaction λ for various values of body rank k in fermion systems with EGOE(1+k). Further, we have shown that the strength function makes transition from Gaussian form to semi-circle form as k changes from 2 to m with sufficiently large λ value and it can be represented by conditional q -normal density described by $f_{CN}(\hat{E}|\hat{\xi} = 0, \zeta, q_H)$ at the center of the spectrum as described in [48]. For $\hat{\xi} \neq 0$, i.e. away from the spectrum, it is clearly seen that the strength functions can also be represented correctly by $f_{CN}(\hat{E}|\hat{\xi}, \zeta, q_H)$ with proper scaling. Similar results were also obtained for bosonic systems in the dense limit [25]. From the results one can see that for $\hat{\xi} \neq 0$ as one moves away from the center of the spectrum, the strength functions become asymmetric and this asymmetry is specifically described by f_{CN} . Going further, the first four moments of the strength function are studied

and utilized to identify the region of thermalization. The numerically computed values of the correlation coefficient ζ , which is related to the width of the strength functions (σ_F), match with the trace propagation results with varying λ for all k values and in the dilute limit $\zeta \rightarrow 0$. Further, we obtain marker λ_t in terms of m , N and k and it is shown that λ_t decreases as the body rank k of interaction increases indicating faster on set of thermalization with k . Further, λ_t obtained via moments of strength functions is in good agreement with the analytical results. Going further, we have studied chaos measure IPR as a function of λ for different values of k and found that the ensemble averaged results are in very good agreement with the two-parameter (q and ζ) formula derived in [25] in the thermalization region ($\lambda \geq \lambda_t$). Results of the present investigation along with obtained in [25, 46–49], it is clear that the q -Hermite polynomials play a very significant role in the analysis of many-body quantum systems interacting via k -body interaction.

ACKNOWLEDGEMENTS

Thanks are due to V. K. B. Kota for many useful discussions. This work is partially supported by Department of Science and Technology (DST), Government of India [Project No.: EMR/2016/001327]. NDC acknowledges financial support from University supported research project [grant No: GCU/RCC/2021-22/20-32/508]. PR acknowledges support from ICTS for participating in the online program - Bangalore School on Statistical Physics XII (Code: ICTS/bssp2021/6).

-
- [1] Znidaric M, Prosen T and Prelovsek P 2008 *Phys. Rev. B* **77** 064426
 - [2] Pal A and Huse D A 2010 *Phys. Rev. B* **82** 174411
 - [3] Khatami E, Rigol M, Relano A and Garcia-Garcia A M 2012 *Phys. Rev. E* **85** 050102(R)
 - [4] Bardarson J H, Pollmann F and Moore J E 2012 *Phys. Rev. Lett.* **109** 017202
 - [5] Nandkishore R and Huse D A 2015 *Ann. Rev. of Condensed Matter Phys.* **6** 15
 - [6] Oganesyan V and Huse D A 2007 *Phys. Rev. B* **75** 155111
 - [7] Altman E and Vosk R 2015 *Ann. Rev. Condens. Matter Phys.* **6** 383
 - [8] Polkovnikov A, Sengupta K, Silva A and Vengalattore M 2011 *Rev. Mod. Phys.* **83** 863
 - [9] Alessio L D, Kafri Y, Polkovnikov A and Rigol M 2016 *Advances in Physics* **65** 239

- [10] Borgonovi F, Izrailev F M, Santos L F and Zelevinsky V G 2016 *Phys. Rep.* **626** 1
- [11] Anderson M, Ensher J, Matthews M, Wieman C and Cornell E 1995 *Science* **269** 198
- [12] Bradley C, Sackett C, Tollett J and Hulet R 1995 *Phys. Rev. Lett.* **75** 1687
- [13] Davis B, Mewes M, Andrews M, Druten N, Durfee D, Kurn D and Ketterle W 1995 *Phys. Rev. Lett.* **75** 3969
- [14] Jordens R et al. 2008 *Nature* **455** 204
- [15] Schneider U et al. 2008 *Science* **322** 1520
- [16] Perfetti et al. 2006 *Phys. Rev. Lett.* **97** 067402
- [17] Cazalilla M A and Rigol M 2010 *New Journal of Physics* **12** 055006
- [18] Rigol M 2009 *Phys. Rev. Lett.* **103** 100403; Rigol M 2009 *Phys. Rev. A* **80** 053607
- [19] Deutsch J M 1991 *Phys. Rev. A* **43** 2046; Srednicki M 1994 *Phys. Rev. E* **50** 888
- [20] Rigol M, Dunjko V and Olshanii M 2008 *Nature* **452** 854
- [21] Santos L F and Rigol M 2010 *Phys. Rev. E* **81** 036206; Santos L F and Rigol M 2010 *Phys. Rev. E* **82** 031130; Rigol M and Santos L F 2010 *Phys. Rev. A* **82** 011604(R)
- [22] Flambaum V V, Izrailev F M and Casati G 1996 *Phys. Rev. E* **54** 2136; Flambaum V V and Izrailev F M 1997 *Phys. Rev. E* **56** 5144
- [23] Borgonovi F and Izrailev F M 2017 *AIP Conference Proceedings* **1912** 020003
- [24] Relano A 2010 *J. Stat. Mech.* **81** P07016
- [25] Rao P and Chavda N D 2021 *Phys. Lett. A* **399** 127302
- [26] Rigol M and Fitzpatrick M 2011 *Phys. Rev. A* **84** 033640
- [27] Santos L F, Borgonovi F and Izrailev F M 2012 *Phys. Rev. Lett.* **108** 094102
- [28] Santos L F, Borgonovi F and Izrailev F M 2012 *Phys. Rev. E* **85** 036209
- [29] Kota V K B and Chavda N D 2018 *Entropy* **20** 541
- [30] Kota V K B, Relano A, Retamosa J and Vyas M 2011 *J. Stat. Mech.* **1** P10028
- [31] Chavda N D, Kota V K B and Potbhare V 2012 *Phys. Lett. A* **376** 2972
- [32] Flambaum V V and Izrailev F M 1997 *Phys. Rev. E* **55** R13
- [33] Kota V K B 2014 *Embedded Random Matrix Ensembles in Quantum Physics* (Heidelberg: Springer)
- [34] Angom D, Ghosh S and Kota V K B 2004 *Phys. Rev. E* **70** 016209
- [35] Vyas M, Kota V K B and Chavda N D 2010 *Phys. Rev. E* **81** 036212
- [36] Flambaum V V, Gribakin G F and Izrailev F M 1996 *Phys. Rev. E* **53** 5729

- [37] Launey K D, Dytrych T and Draayer J P 2012 *Phys. Rev. C* **85** 044003
- [38] Blatt D W E and McKellar B H J 1975 *Phys. Rev. C* **11** 2040
- [39] Hammer H W, Nogga A and Schwenk A 2013 *Rev. Mod. Phys.* **85** 197
- [40] Ortega A, Vyas M and Benet L 2015 *Ann. Phys. (Berlin)* **527** 748
- [41] Ortega A, Stegmann T and Benet L 2016 *Phys. Rev. E* **94** 042102
- [42] Ortega A, Stegmann T and Benet L 2018 *Phys. Rev. E* **98** 012141
- [43] Cotler J S et al. 2017 *J. High Energy Phys.* **05** 118
- [44] Garcia-Garcia A M, Jia Y and Verbaarschot J J M 2018 *Phys. Rev. D* **97** 106003
- [45] Garcia-Garcia A M, Nosaka T, Rosa D and Verbaarschot J J M 2019 *Phys. Rev. D* **100** 026002
- [46] Vyas M and Kota V K B 2019 *J. Stat. Mech.* **10** 103103
- [47] Kota V K B and Vyas M 2020 *J. Stat. Mech.* 093101/1-17
- [48] Kota V K B and Vyas M 2021 *J. Stat. Mech.* 113103/1-25
- [49] Chavda N D 2022 *Pramana – J. Phys.* **96** 223
- [50] Mon K K and French J B 1975 *Ann. Phys., NY* **95** 90
- [51] Brody T A, Flores J, French J B, Mello P A, Pandey A and Wong S S M 1981 *Rev. Mod. Phys.* **53** 385
- [52] Garcia-Garcia A M and Verbaarschot J J M 2017 *Phys. Rev. D* **96** 066012
- [53] Garcia-Garcia A M and Verbaarschot J J M 2016 *Phys. Rev. D* **94** 126010
- [54] Szablowski P 2010 *Electronic Journal of Probability* **15** 1296
- [55] Chavda N D and Kota V K B 2017 *Ann. Phys. (Berlin)* **529** 1600287
- [56] Ismail M E H, Stanton D and Viennot G 1987 *Europ. J. Combinatorics* **8** 379
- [57] Szablowski P 2013 *Demonstratio Math.* **46** 679
- [58] Raza N, Fadel M, Nisar K S and Zakarya M 2021 *AIMS Mathematics* **6(8)** 8705
- [59] Chavda N D, Potbhare V and Kota V K B 2004 *Phys. Lett. A* **326** 47
- [60] Lauritzen B, Bortignon P F, Broglia R A and Zelevinsky V G 1995 *Phys. Rev. Lett* **74** 5190
- [61] Jacquod Ph. and Varga I A 2002 *Phys. Rev. Lett.* **89** 134101
- [62] Angom D, Ghosh S and Kota V K B 2004 *Phys. Rev. E* **70** 016209

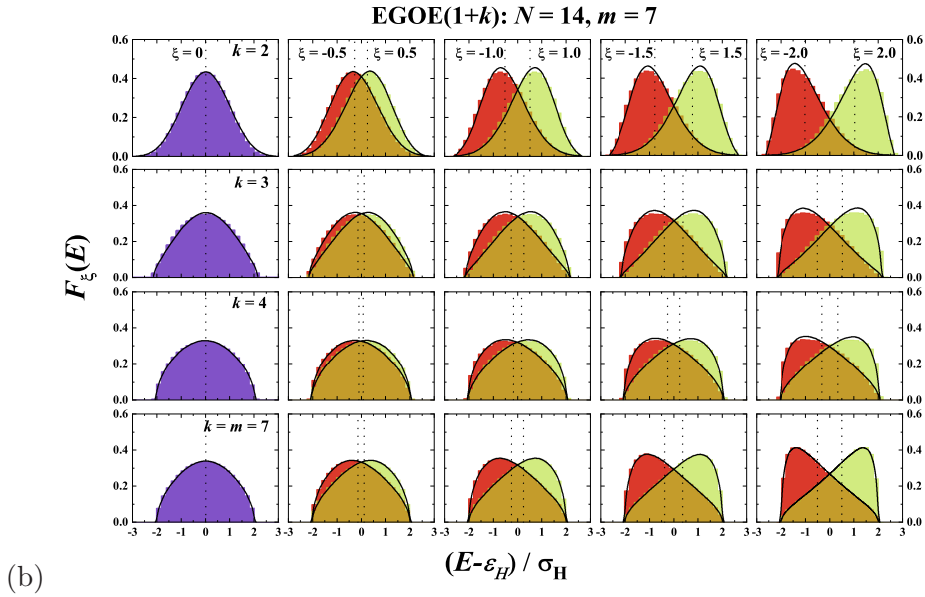
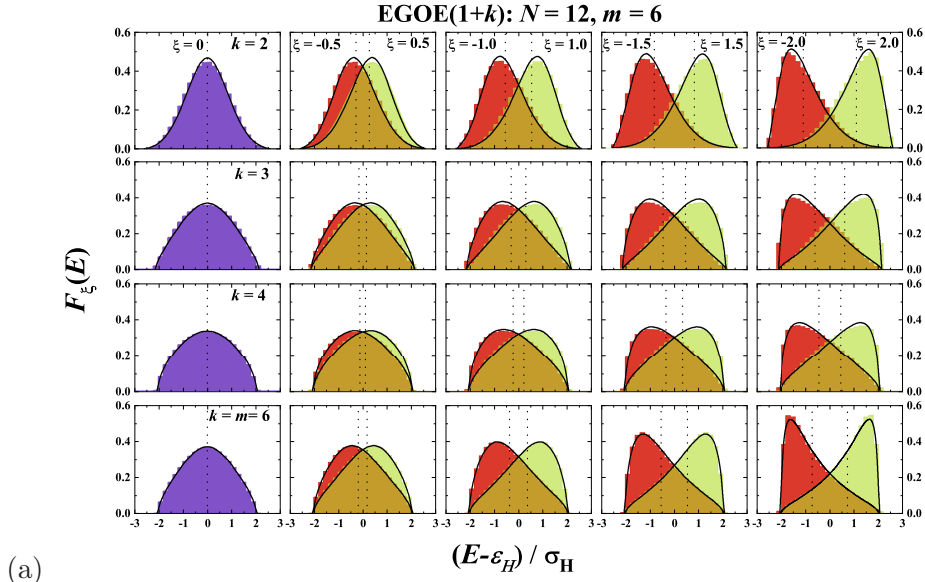


FIG. 5. Ensemble averaged strength function as a function of normalized energy E for (a) a 100 member EGOE(1+k) ensemble with $m = 6$ and $N = 12$ and (b) a 20 member EGOE(1+k) ensemble with $m = 7$ and $N = 14$. Results are shown for $k=2,3,4$ and $k = m$ and $\lambda = 0.5$ is chosen for both the examples. Histograms in extreme left panels correspond to strength functions for $\xi = 0$ and histograms in the remaining panels correspond to strength functions for $\xi = \pm 0.5, \pm 1.0, \pm 1.5$ and ± 2.0 . In the plots $\int F_\xi(E) dE = 1$. The continuous curves are due to fitting with $f_{CN}(\hat{E}|\hat{\xi}; \zeta, q = q_H)$ given by equation 7 with corresponding ensemble averaged q_H and ζ values. The vertical dotted lines, in each panel, correspond to centroid, $\epsilon_F = \zeta \xi$. See text for more details.

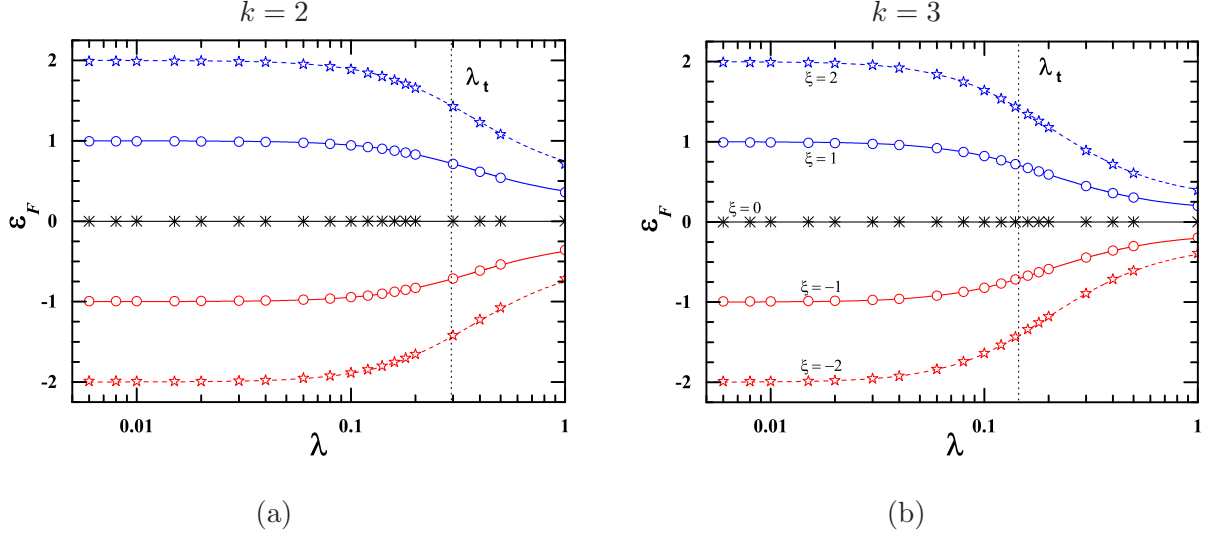


FIG. 6. Centroid of the strength functions vs. λ for the example of 100 member EGOE(1+k) with $m=6$ fermions in $N=12$ sp states for (a) $k=2$ and (b) $k=3$. The results are shown for various values of ξ . For more details refer the text.

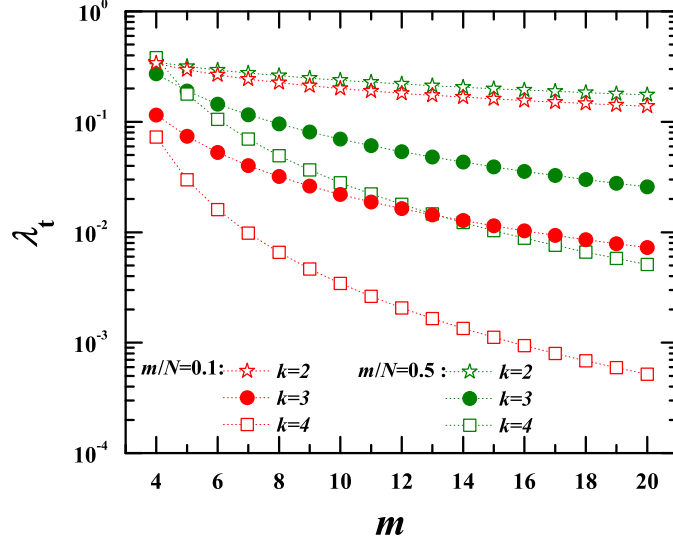


FIG. 7. Marker λ_t vs. m for fermion systems. Results are obtained using equation 19 for $k=2,3$ and 4 and for various values of m/N .

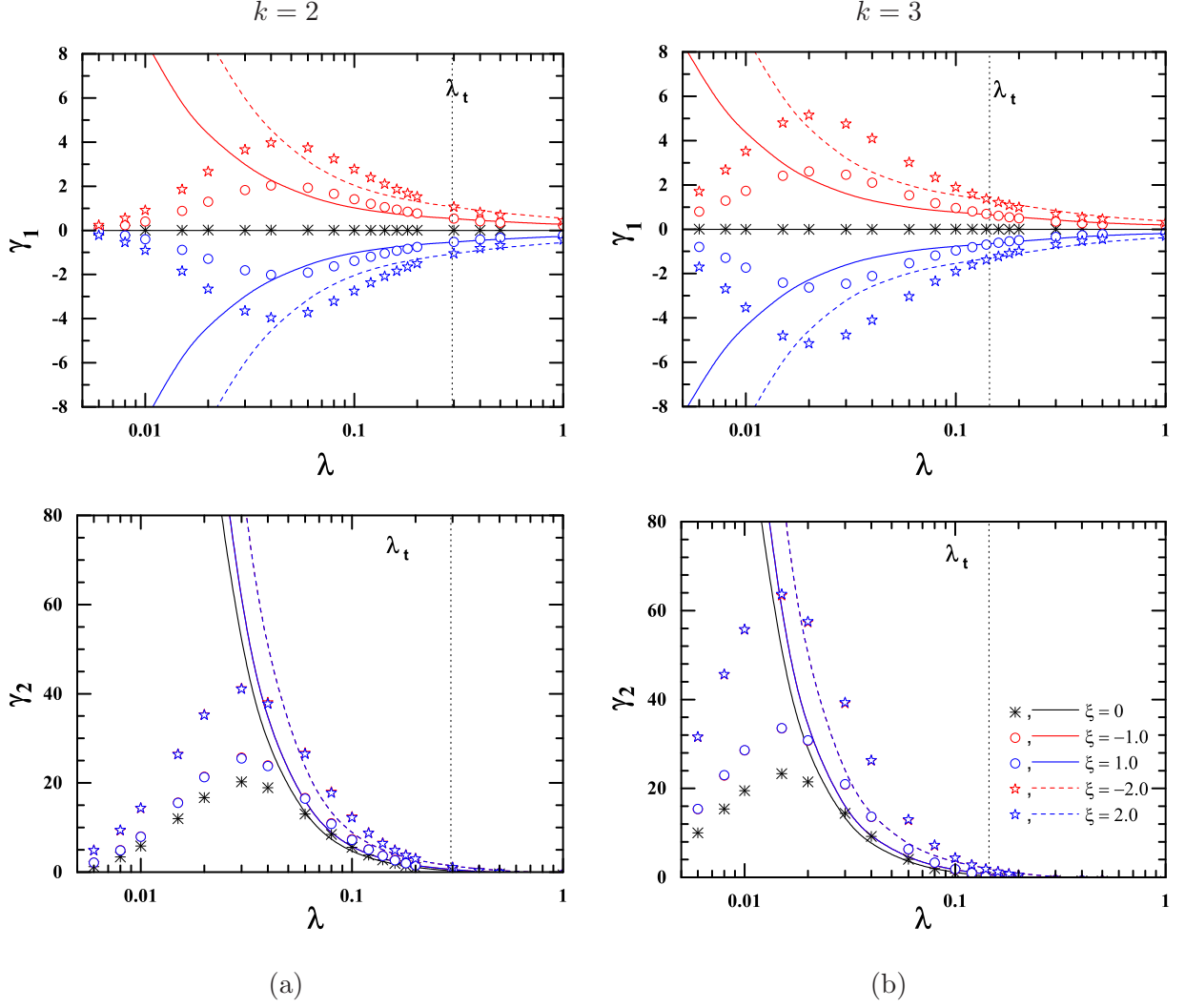


FIG. 8. Variation of γ_1 and γ_2 of strength functions as a function of λ . The results are shown for various values of ξ for the example of 100 member EGOE($1+k$) with $m=6$ fermions in $N=12$ sp states for (a) $k = 2$ and (b) $k = 3$. The vertical dotted lines in each panel indicate position of λ_t . For details refer the text.

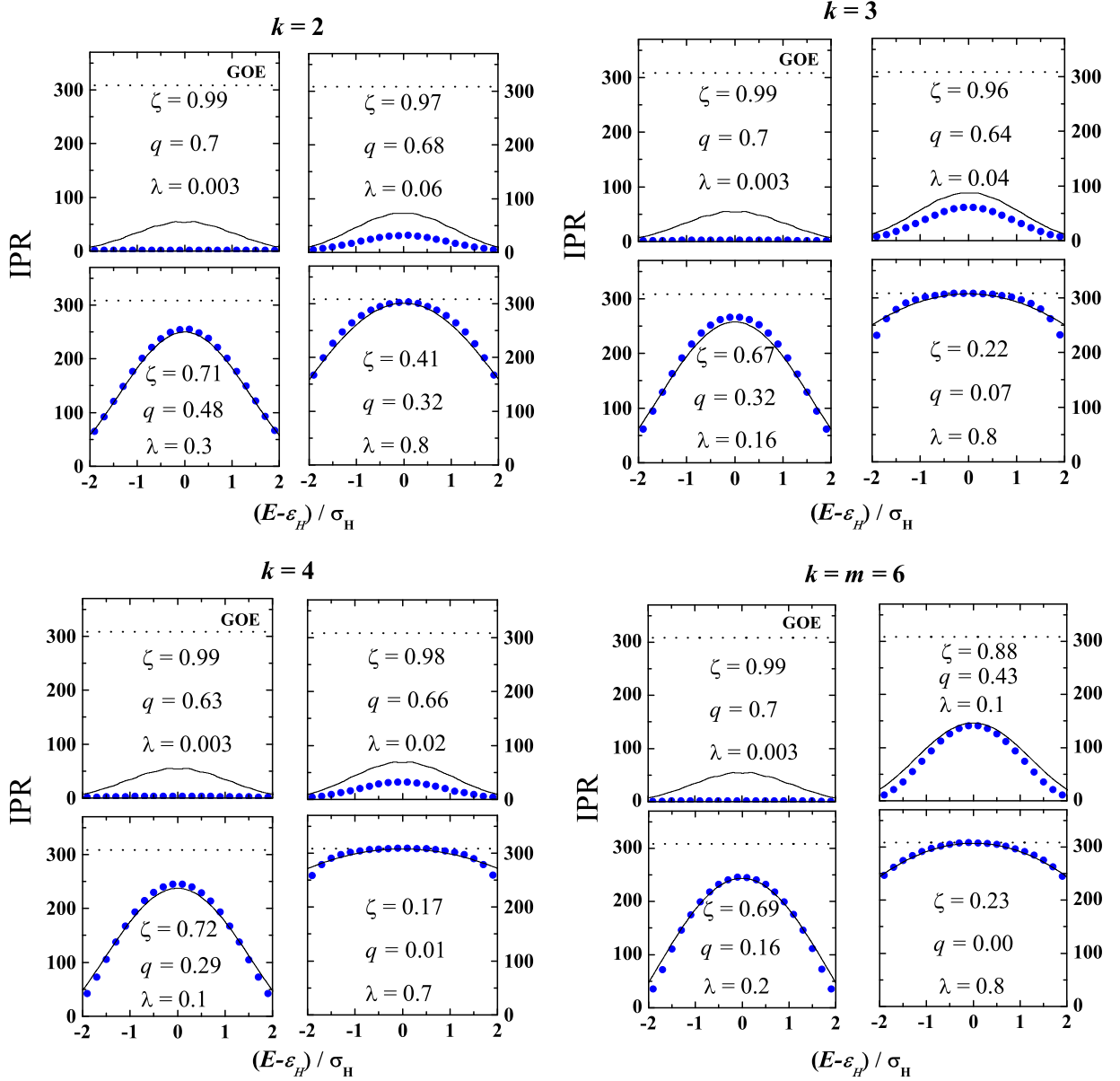


FIG. 9. Ensemble averaged IPR as a function of normalized energy E for EGOE(1+k) with $m = 6$ fermions distributed in $N = 12$ sp states for body rank $k = 2, 3, 4$ and $k = m = 6$. Here an ensemble of 100 members is considered. Results are shown for various values of λ . Here blue solid circles correspond to numerical ensemble averaged EGOE(1+k) results and the continuous black curves correspond to theoretical curves obtained via equation 22. GOE estimate is shown by dotted lines in each graph.